Local ionic liquid environment at a modified iron porphyrin catalyst enhances the electrocatalytic performance of CO2 to CO reduction in water

Asma Khadhraoui, Philipp Gotico, Bernard Boitrel, Winfried Leibl, Zakaria Halime, Ally Aukauloo

Local ionic liquid environment at a modified iron porphyrin catalyst enhances the electrocatalytic performance of CO_2 to CO reduction in water†

Asma Khadhraoui,[a] Philipp Gotico, [b] Bernard Boitrel, [c] Winfried Leibl,[b] Zakaria Halime*[a] and Ally Aukauloo *[ab]

In this study we report a strategy to attach methylimidazolium fragments as ionic liquid units on an established iron porphyrin catalyst for the selective reduction of CO_2 to CO. Importantly, we found that the tetra-methylimidazolium containing porphyrin exhibits an exalted electrocatalytic activity at low overpotential in water precluding the need for an external proton donor.

During natural photosynthesis, nature extracts electrons and protons from water thereby releasing dioxygen. These electrons and protons are then used to fix carbon from its most oxidized form (CO_2) to energy rich molecules (sugars). In the actual context of searching for new sustainable ways to produce energy and mitigate climatic constraints, scientists are aiming to convert carbon dioxide to a fuel or to use it as a synthetic C1 unit in chemical transformations. Because of the high energetic barrier to activate CO_2 and the variety of reduced products that can be formed, there is an urgent need to discover new, efficient, and selective catalysts.[1–6]

Molecular chemistry offers many handles to implement several tactics for the development and optimization of catalysts.[7–16] Iron porphyrin derivatives have been shown to be highly performing catalysts for the reduction of CO_2 to CO.[17,18] Hinging on this finding, development of more sophisticated porphyrin macrocycles holding functional groups such as proton donors or cationic units in the second coordination sphere has contributed to lowering the overpotential of this energetically demanding reaction and also to enhancing the

catalytic turnover numbers and frequencies.[19–21] However, a recent finding that zinc porphyrins can also manage the reduction of CO_2 to CO has brought new perspectives in considering the redox participation of the porphyrin macrocycle in the observed catalytic reactivity.[22] Put together, all these results are supportive of the fact that this quest is gathering considerable momentum on the way towards a better understanding and optimization of catalysts for the selective reduction of CO_2.

Masel and colleagues first reported the use of ionic liquids (IL) to shift the overpotential for the reduction of CO_2 to more positive values in a heterogeneous electrocatalysis system.[23] The effect of the IL was attributed to the stabilization of the one-electron-reduced $CO_2^{\bullet-}$ species by the methylimidazolium units, thereby facilitating further reduction. Implementation of the ionic liquid as a cofactor in both homogeneous and heterogeneous catalysis has demonstrated a beneficial role in the catalytic processes. The ionic liquid was shown to shift the reduction potential of the active form of iron porphyrin developed by Robert, Costentin and Savéant (RCS) to more positive values and to enhance the kinetics of CO_2 reduction.[24]

However, most electrocatalytic studies were realized in organic solvents and in the presence of a sacrificial proton donor (trifluoroethanol). More recently, a methylimidazolium-functionalized rhenium (Lehn's type) catalyst was also reported with improved electrocatalytic properties.[25] Intriguingly, addition of water as a proton source resulted in a significant increase of the catalytic current at lower overpotential, but at higher concentrations of water, a drastic drop in the catalytic current together with positive potential shifts was observed. It must be pointed out that no detailed mechanistic studies are yet available to explain the positive effects of the use of ionic liquids to perform the selective two-electron and two-proton reduction of CO_2 to CO ($CO_2 + 2e^- + 2H^+ \rightarrow CO + H_2O$).

With these interrogations in mind, we have been interested in investigating the electrocatalytic properties of an iron porphyrin derivative with attached methylimidazolium units on

[a] Institut de Chimie Moléculaire et des Matériaux d'Orsay (UMR CNRS 8182),
Université Paris-Sud, Bat 420, Rue Doyen G. Poitou, Orsay, 91405, France.
E-mail: zakaria.halime@u-psud.fr, ally.aukauloo@u-psud.fr
[b] Laboratoire des Mécanismes fondamentaux de la Bioénergétique (LMB),
Institut de Biologie Intégrative de la Cellule (I2BC), Institut des Sciences
du Vivant Frédéric-Joliot, CEA Saclay, Gif-sur-Yvette 91191, France
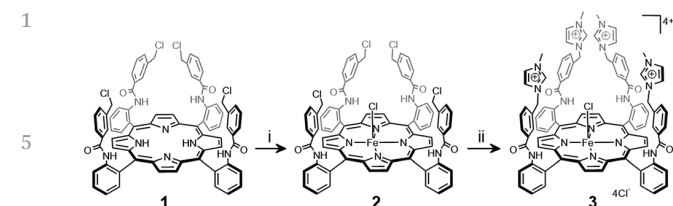[c] Univ Rennes, CNRS, ISCR (Institut des Sciences Chimiques de Rennes),
UMR 6226, Rennes F-35000, France
† Electronic supplementary information (ESI) available: Details of materials and
methods are available. See DOI: 10.1039/c8cc06475j

Scheme 1 Synthesis of iron porphyrin catalyst **3** bearing four methylimi-dazolium groups. (i) FeCl$_2$, 2,6-lutidine, and THF at RT and (ii) 1-methylimidazol, DMF at 70 °C.

the periphery of the porphyrin macrocycle. For this study, we have prepared an iron complex of an α-4-tetraimidazolium tetraphenylporphyrin ligand as depicted in Scheme 1. Inspiration for the targeted catalyst stems from the pioneering work of Collman and Boitrel where the semi-rigid "U-shaped" aryl–amide–aryl motif in porphyrin **1** was used to introduce coordinating or functional groups in a pre-organized fashion close to the coordination sphere of the metal ion lying in the center of the porphyrin ring.[26–29] Complex **3** was prepared in two steps based on the previous description of porphyrin **1**.[27] In the first step, an iron(II) ion was inserted in the N4 coordinating cavity of the porphyrin macrocycle using ferrous chloride in the presence of a base. The substitution of the chloro groups at the benzylic positions was realized upon treatment with stoichiometric amounts of N-methylimidazole at 70 °C to prevent the formation of rotational isomers. The synthetic procedures and characterization of the studied complexes are given in the ESI.†

Cyclic voltammetry (CV) of complex **3** in an argon-degassed DMF/H$_2$O 9∶1 mixture containing 0.1 M of tetra-N-butyl-ammonium hexafluorophosphate (TBAPF$_6$) showed three reversible waves in the cathodic region at +0.10, −0.73, and −1.04 V *vs.* NHE corresponding respectively to the formal Fe^{III}/Fe^{II}, Fe^{II}/Fe^{I} and Fe^{I}/Fe^0 couples (Fig. 1). However, recent reports suggest that the second and the third redox waves mainly concern the porphyrin core acting as the locus for the addition of the two supplementary electrons and therefore can be formulated as Fe^{II}porph/Fe^{II}porph$^{\bullet-}$ and Fe^{II}porph$^{\bullet-}$/Fe^{II}porph$^{\bullet\bullet2-}$ couples (porph = porphyrin).[30,31] With the aim to provide a comparative reference, we have investigated, under similar experimental conditions, the non-functionalized iron tetraphenylporphyrin (**FeTPP**) together with the **FeTPPF$_8$** and the **FeTPPF$_{20}$** derivatives (see Fig. 1). The standard potentials of the iron complexes are gathered in Table S1 (in the ESI†). The first important comparison concerns the Fe$^{III/II}$ couple. As we can notice, from the **FeTPP**, **FeTPPF$_8$** and **FeTPPF$_{20}$** derivatives, the reduction potentials shift to more anodic values, in agreement with the electron withdrawing effect of the fluoro groups. Interestingly, we found that the standard potential for the Fe$^{III/II}$ couple for **3** is not affected by the presence of the four methylimidazolium groups. This observation therefore rules out a direct inductive effect of the positively charged units on the ligand strength of the N4 coordinating cavity of the porphyrin macrocycle. However, the CV of **3** displays a shift of *ca.* 120 and 415 mV towards more
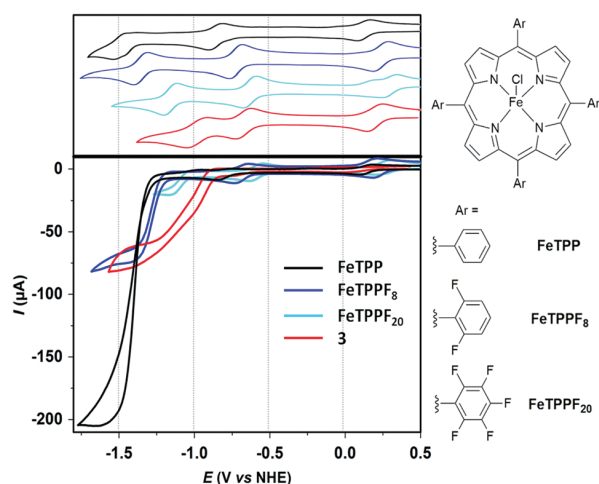

Fig. 1 Cyclic voltammetry of **FeTPP**, **FeTPPF$_8$**, **FeTPPF$_{20}$** and **3** (1 mM) in DMF/H$_2$O 9∶1 containing 0.1 M of tetra-N-butylammonium hexafluoro-phosphate (TBAPF$_6$) at 25 °C under Ar (upper left) and CO$_2$ (lower left) atmospheres. Structures of the three reference iron porphyrins are shown in the right.

positive potentials, in comparison with **FeTPP**, for the second and third waves, respectively (Fig. 1 and Table S1 in the ESI†). As we can notice, the third wave is more drastically affected than those of the modified **FeTPP** bearing 8 (**FeTPPF$_8$**) or 20 (**FeTPPF$_{20}$**) fluorine atoms as electron-withdrawing groups (Fig. 1). We attribute this significant shift to the stabilization of the dianionic reduced form of the iron porphyrin through a space-charge interaction with the positively charged methyl-imidazolium groups. This strategy therefore provides convincing support that the topologically pre-organized aryl–amide–aryl arms bring the methylimidazolium groups close to the porphyrin platform and help to support charge accumulation. The electrocatalytic properties of the set of iron porphyrins were examined by performing CV under a CO$_2$ atmosphere in DMF, with water (10%) acting as the proton source. The **FeTPPF$_8$** presents an onset potential for the electrocatalytic reduction of CO$_2$ at around −1.27 V. This E_{cat}^0 falls within the potential window for differently substituted iron tetra-aryl porphyrins and follows the iron law proposed by RCS (see above),[32] which states that gains in the form of smaller over-potential come at the price of a slower reaction, illustrated by a smaller catalytic current. Under a CO$_2$ atmosphere, **3** presents a catalytic wave for CO$_2$ reduction at $E_{cat}^0 = -1.05$ V *vs.* NHE, a value 375 mV more positive than that of **FeTPP** under the same experimental conditions (Fig. 1 and Table S1, ESI†). Of note, this onset potential corresponds to one of the lowest over-potentials $\eta = 366$ mV ($\eta = E_{(CO_2/CO)}^0 - E_{cat}^0$ with $E_{(CO_2/CO)}^0 = -0.69$ V *vs.* NHE) reported in the literature for CO$_2$ reduction by metalloporphyrin catalysts. Remarkably, even at this low over-potential, the catalytic current observed for **3** is comparable to that of **FeTPPF$_8$** exhibiting an E_{cat}^0 at *ca.* 220 mV more cathodic values.

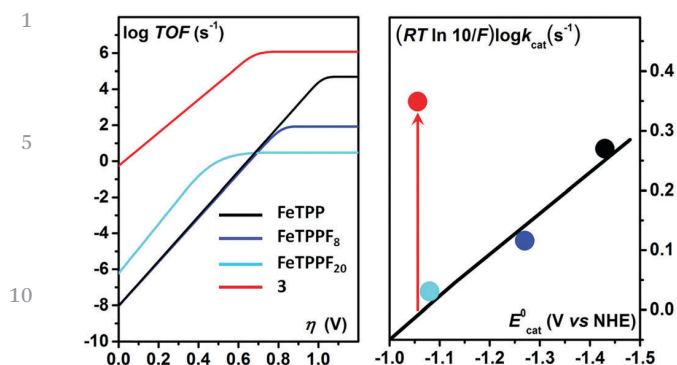With the aim to benchmark the electrochemical performance observed for **3**, two diagrams introduced by

Fig. 2 Catalytic Tafel plots of **FeTPP**, **FeTPPF$_8$**, **FeTPPF$_{20}$** and **3** in DMF/H$_2$O 9 : 1 (left) and correlation plots between $(RT \ln 10/F)\log k_{cat}$ and E_{cat}^0 (right) (see details in the ESI†).

Fig. 3 Cyclic voltammetry of 0.5 mM solution of **FeTPP** (black) and **3** (red) in DMF/H$_2$O 9 : 1 containing 0.1 M of TBAPF$_6$ and cyclic voltammetry of 0.5 mM solution of **3** in water containing 0.1 M of KCl (magenta) at 25 °C under a CO$_2$ atmosphere.

RCS,[21,32–35] were drawn for the four complexes (Fig. 2). The first is the Tafel plots expressing the electrochemical turnover frequency (TOF) *vs.* overpotential (η), and the second is the $(RT \ln 10/F)\log k_{cat}$ *vs.* E_{cat}^0 plots which illustrate the electronic effect of the porphyrin substituent on the electrocatalysis and can reveal through-space activation. As expected from the CVs (Fig. 1), complex **3** is a much better catalyst than the other three complexes as indicated by the significant shift of its Tafel plot to the upper left side of the diagram (Fig. 2, left). Catalyst **3** is also characterized by an upper left deviation from the linear correlation of $(RT \ln 10/F)\log k_{cat}$ *vs.* E_{cat}^0,[32] sustained by the three other catalysts. From the analysis of these two diagrams, and in contrast with the classical strategy to modulate catalytic properties by electronic inductive effects, we can conclude that the enhanced catalytic activity of **3** can be due to a through-space electrostatic interaction between the methylimidazolium groups and the reduced iron/substrate catalytic intermediates.

In a control experiment, the CV of a 1-benzyl-3-methylimidazolium chloride fragment under the same conditions under a CO$_2$ atmosphere shows no catalytic current (Fig. S1, ESI†). The addition of four equivalents of 1-benzyl-3-methylimidazolium chloride during the catalytic reduction of CO$_2$ by **FeTPP** does not enhance the catalytic activity (Fig. S1, ESI†). Thus, the enhanced catalytic activity of **3** can largely be attributed to a synergistic action of the attached methylimidazolium arms and the iron porphyrin core. Additional stabilization from hydrogen bonding interactions with the four amide functions on the *ortho* position of the aryl groups can also participate to a lesser extent in the observed increase in the electrocatalytic activity as it was recently reported by the group of Chang.[36]

The tetracationic nature of **3** renders it water-soluble hence allowing us to evaluate its catalytic performance for CO$_2$ reduction in water as a convenient and clean solvent and a proton source. The CV of **3** in Ar-degassed water containing 0.1 M potassium chloride (KCl) shows three redox processes similar to those observed in DMF (Table S1, ESI†). However, even though CO$_2$ is less soluble in water (0.033 M) than in DMF (0.23 M), the CV displays a much higher catalytic current for
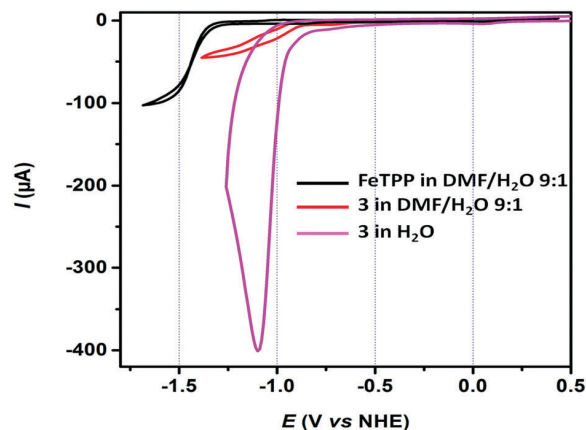
CO$_2$ reduction at a potential as low as $E_{cat}^0 = -1.018$ V *vs.* NHE (Fig. 3). To explain this higher catalytic activity in water, we have to take into consideration the primary intermediate proposed for CO$_2$ reduction by iron porphyrins which is [Fe(porphyrin)CO$_2$]$^{2-}$ described formally as a resonance of Fe^I(CO$_2^{\bullet-}$) and Fe^{II}(CO$_2^{2-}$).[32,37,38] As described earlier, the positive deviation from the expected electrochemical reactivity as already observed in DMF may be assigned to the stabilization of this intermediate through Coulombic interactions with the positive charges of the methylimidazolium groups. In water, which has a higher relative permittivity (ε_r(H$_2$O) = 78.4) compared to DMF (ε_r(DMF) = 36.7),[39] the degree of dissociation of the attached ionic liquid (methylimidazolium$^+$Cl$^-$) units is greater than that in DMF,[40] which leads to better stabilization of the [Fe(porphyrin)CO$_2$]$^{2-}$ adduct through stronger space-charge interactions with more "free" methylimidazolium groups.

The linear dependence of the peak current on the square root of the scan rate indicates a diffusion-controlled homogenous process (Fig. S4, ESI†). After electrocatalytic runs, the electrode was rinsed and transferred to a fresh solution of electrolyte. No electrocatalytic feature was observed bringing support for the homogeneous nature of the catalytic process, in line with those of other **FeTPP** derivatives.

Gas chromatography analysis of the electrochemical reaction headspace during bulk electrolysis experiments was performed to examine the selectivity and the efficiency of catalyst **3** for CO$_2$ reduction in water. As shown in Fig. 4, 2 hours of electrocatalysis at $E_{electrolysis} = -0.948$ V *vs.* NHE, which corresponds to an overpotential of 418 mV ($E_{(CO_2/CO)}^0 = -0.53$ V *vs.* NHE in H$_2$O), and a current density of 1.06 mA cm^{-2}, led to the exclusive formation of CO with 91% faradaic efficiency (no H$_2$ or HCO$_2$H were detected). Considering a two-electron process, the rate constant (k_{cat}), TOF and TON values of 2.44 × 10^5 s^{-1}, 14986 s^{-1} (log TOF = 4.18) and 1.08 × 10^8 were respectively calculated for **3** (see the ESI†) based on the catalyst molecules in the diffusion layer at the cathode. It is to be stressed that these
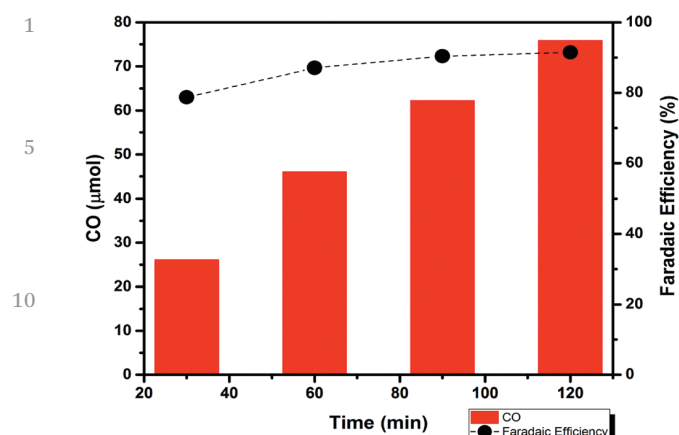
Fig. 4 CO evolution trace and the corresponding faradaic efficiency in bulk electrolysis experiments in the presence of catalyst **3** (0.5 mM) at −0.948 V *vs.* NHE in water containing 0.1 M KCl at 25 °C under a CO_2 atmosphere.

electrocatalytic parameters obtained in water as a solvent and a proton donor are higher than those reported for **FeTPP** in DMF with 1 M of tetrafluoroethanol as a proton source and 0.3 M of methylimidazolium-type ionic liquid at 870 mV overpotential.[24]

In conclusion, we have introduced methylimidazolium groups on the periphery of an iron porphyrin (**3**) to provide a confined pre-organized ionic liquid environment. This modification led not only to a beneficial anodic shift for the addition of electrons but also to an enhanced electrocatalytic two-electron reduction of CO_2 to CO in DMF. No marked changes in the electrocatalytic activity were noticed in a bimolecular mixture where an exogenous ionic liquid component was added to a reference iron porphyrin derivative. More importantly, the electrocatalytic activity of **3** in water, as a solvent and a sole proton source, was even higher with an excellent selectivity for CO production at low overpotential. Hence, these results reinforce the strategy that meticulous design and manipulation of the second coordination sphere, in this particular case through-space electrostatic interactions, can promote the reduction of the CO_2 substrate to CO by iron porphyrins.

Conflicts of interest

There are no conflicts to declare.

Notes and references

1 M. Aresta, A. Dibenedetto and A. Angelini, *Chem. Rev.*, 2014, **114**, 1709–1742.
2 Q. Liu, L. Wu, R. Jackstell and M. Beller, *Nat. Commun.*, 2015, **6**, 5933.
3 M. Aresta, *Carbon Dioxide as Chemical Feedstock*, Wiley, 2010.
4 A. M. Appel, J. E. Bercaw, A. B. Bocarsly, H. Dobbek, D. L. DuBois, M. Dupuis, J. G. Ferry, E. Fujita, R. Hille, P. J. A. Kenis, C. A. Kerfeld, R. H. Morris, C. H. F. Peden, A. R. Portis, S. W. Ragsdale, T. B. Rauchfuss, J. N. H. Reek, L. C. Seefeldt, R. K. Thauer and G. L. Waldrop, *Chem. Rev.*, 2013, **113**, 6621–6658.
5 M. Cokoja, C. Bruckmeier, B. Rieger, W. A. Herrmann and F. E. Kühn, *Angew. Chem., Int. Ed.*, 2011, **50**, 8510–8537.
6 S. C. Roy, O. K. Varghese, M. Paulose and C. A. Grimes, *ACS Nano*, 2010, **4**, 1259–1278.
7 J. Hawecker, J.-M. Lehn and R. Ziessel, *J. Chem. Soc., Chem. Commun.*, 1983, 536–538.
8 H. Takeda, C. Cometto, O. Ishitani and M. Robert, *ACS Catal.*, 2017, **7**, 70–88.
9 D. Hong, Y. Tsukakoshi, H. Kotani, T. Ishizuka and T. Kojima, *J. Am. Chem. Soc.*, 2017, **139**, 6538–6541.
10 Y. Tamaki and O. Ishitani, *ACS Catal.*, 2017, **7**, 3394–3409.
11 T. Ouyang, H.-H. Huang, J.-W. Wang, D.-C. Zhong and T.-B. Lu, *Angew. Chem., Int. Ed.*, 2017, **56**, 738–743.
12 F. Wang, *ChemSusChem*, 2017, **10**, 4393–4402.
13 J.-W. Wang, W.-J. Liu, D.-C. Zhong and T.-B. Lu, *Coord. Chem. Rev.*, DOI: 10.1016/j.ccr.2017.12.009.
14 M. Stanbury, J.-D. Compain and S. Chardon-Noblat, *Coord. Chem. Rev.*, 2018, **361**, 120–137.
15 C. Cometto, L. Chen, P.-K. Lo, Z. Guo, K.-C. Lau, E. Anxolabéhère-Mallart, C. Fave, T.-C. Lau and M. Robert, *ACS Catal.*, 2018, **8**, 3411–3417.
16 K. M. Waldie, F. M. Brunner and C. P. Kubiak, *ACS Sustainable Chem. Eng.*, 2018, **6**, 6841–6848.
17 M. Hammouche, D. Lexa, J. M. Savéant and M. Momenteau, *J. Electroanal. Chem. Interfacial Electrochem.*, 1988, **249**, 347–351.
18 M. Hammouche, D. Lexa, M. Momenteau and J. M. Saveant, *J. Am. Chem. Soc.*, 1991, **113**, 8455–8466.
19 C. Costentin, S. Drouet, M. Robert and J.-M. Savéant, *Science*, 2012, **338**, 90–94.
20 R. B. Ambre, Q. Daniel, T. Fan, H. Chen, B. Zhang, L. Wang, M. S. G. Ahlquist, L. Duan and L. Sun, *Chem. Commun.*, 2016, **52**, 14478–14481.
21 I. Azcarate, C. Costentin, M. Robert and J.-M. Savéant, *J. Am. Chem. Soc.*, 2016, **138**, 16639–16644.
22 Y. Wu, J. Jiang, Z. Weng, M. Wang, D. L. J. Broere, Y. Zhong, G. W. Brudvig, Z. Feng and H. Wang, *ACS Cent. Sci.*, 2017, **3**, 847–852.
23 B. A. Rosen, A. Salehi-Khojin, M. R. Thorson, W. Zhu, D. T. Whipple, P. J. A. Kenis and R. I. Masel, *Science*, 2011, **334**, 643–644.
24 J. Choi, T. M. Benedetti, R. Jalili, A. Walker, G. G. Wallace and D. L. Officer, *Chem. – Eur. J.*, 2016, **22**, 14158–14161.
25 S. Sung, D. Kumar, M. Gil-Sepulcre and M. Nippe, *J. Am. Chem. Soc.*, 2017, **139**, 13993–13996.
26 J. P. Collman, R. R. Gagne, C. Reed, T. R. Halbert, G. Lang and W. T. Robinson, *J. Am. Chem. Soc.*, 1975, **97**, 1427–1439.
27 A. Didier, L. Michaudet, D. Ricard, V. Baveux-Chambenoît, P. Richard and B. Boitrel, *Eur. J. Org. Chem.*, 2001, 1927–1926.
28 Z. Halime, M. Lachkar, T. Roisnel, E. Furet, J.-F. Halet and B. Boitrel, *Angew. Chem., Int. Ed.*, 2007, **46**, 5120–5124.
29 I. Hijazi, T. Roisnel, P. Even-Hernandez, E. Furet, J.-F. Halet, O. Cador and B. Boitrel, *J. Am. Chem. Soc.*, 2010, **132**, 10652–10653.
30 C. Römelt, J. Song, M. Tarrago, J. A. Rees, M. van Gastel, T. Weyhermüller, S. DeBeer, E. Bill, F. Neese and S. Ye, *Inorg. Chem.*, 2017, **56**, 4745–4750.
31 A. J. Göttle and M. T. M. Koper, *J. Am. Chem. Soc.*, 2018, **140**, 4826–4834.
32 C. Costentin and J.-M. Savéant, *Nat. Rev. Chem.*, 2017, **1**, 0087.
33 C. Costentin, M. Robert and J.-M. Savéant, *Acc. Chem. Res.*, 2015, **48**, 2996–3006.
34 V. Artero and J.-M. Saveant, *Energy Environ. Sci.*, 2014, **7**, 3808–3814.
35 C. Costentin and J.-M. Savéant, *J. Am. Chem. Soc.*, 2017, **139**, 8245–8250.
36 E. M. Nichols, J. S. Derrick, S. K. Nistanaki, P. T. Smith and C. J. Chang, *Chem. Sci.*, 2018, **9**, 2952–2960.
37 C. Costentin, S. Drouet, G. Passard, M. Robert and J.-M. Savéant, *J. Am. Chem. Soc.*, 2013, **135**, 9023–9031.
38 B. Mondal, A. Rana, P. Sen and A. Dey, *J. Am. Chem. Soc.*, 2015, **137**, 11214–11217.
39 K. Izutsu, in *Electrochemistry in Nonaqueous Solutions*, Wiley-Blackwell, 2003, pp. 167–200.
40 W. Li, Z. Zhang, B. Han, S. Hu, Y. Xie and G. Yang, *J. Phys. Chem. B*, 2007, **111**, 6452–6456.